OLDHAMITE IN ENSTATITE ACHONDRITES (AUBRITES)

Katharina LODDERS

Planetary Chemistry Laboratory,
Department of Earth and Planetary Sciences, Washington University, Campus Box 1169,
One Brookings Drive, St. Louis, MO 63130-4899, U. S. A.

Abstract: Properties of oldhamite (ideally CaS) in aubrites are summarized and compared to oldhamite in enstatite chondrites. The origin of the high REE abundances in aubritic oldhamite and the diversity of REE abundance patterns is addressed. Low CaS/silicate partition coefficients indicate that oldhamite in enstatite achondrites cannot have gained its high REE concentrations during igneous differentiation processes. However, the observed REE abundance patterns in oldhamite can be explained by REE condensation into CaS grains in the solar nebula. The very high melting point of oldhamite plausibly led to its preservation and prevented major exchange reactions of the oldhamite with other aubritic minerals during the short differentiation and metamorphism period on the aubrite parent body. Thus, oldhamite in aubrites is probably a slightly metamorphosed relict condensate, as suggested earlier.

1. Introduction

The mineralogy and chemistry of the highly reduced enstatite chondrites and enstatite achondrites (aubrites) are distinctive compared to that of other meteorite types and terrestrial rocks (MASON, 1966; KEIL, 1968). Table 1 lists some of the minerals observed in the primitive EH and EL chondrites as well as in aubrites, which are silicate rocks from a differentiated parent body. The occurrence of some of the exotic sulfides and metallic phases is explained by the formation of these meteorites under highly reducing conditions. Highly reducing conditions imply that oxygen was depleted and lithophile elements, which are normally observed in oxide and silicate phases, occur (partially) as sulfides (Fe, Mg, Mn, Ca, Ti, REE), as nitrides (Si, Ti), or alloyed with metallic FeNi (*e.g.*, Si).

Among the sulfide phases, oldhamite (ideal formula CaS) is of particular interest for two reasons. First, pure CaS is very refractory with a melting point of 2450°C. It is calculated (LARIMER, 1975; LARIMER and BARTHOLOMAY, 1979; LODDERS and FEGLEY, 1993) to be among the first condensates in a reduced solar gas (for C/O>1, CaS condenses at 1379 K at 10^{-3} bars total pressure). Thus, oldhamite is analogous to hibonite ($CaAl_{12}O_{19}$) and perovskite ($CaTiO_3$) the two most refractory Ca-bearing phases in Ca,Al-rich inclusions in carbonaceous chondrites (*e.g.*, KORNACKI and FEGLEY, 1984, 1986).

Second, oldhamite is an important host phase for the rare earth elements (REE) in enstatite chondrites and achondrites. Typically, REE abundances in oldhamite are about 100 times CI-chondritic and a variety of REE abundance patterns are observed (*e.g.*, LARIMER and GANAPATHY, 1987; FLOSS *et al.*, 1990; LODDERS and PALME 1991; KURAT *et al.*, 1992; FLOSS and CROZAZ, 1993; LODDERS *et al.*, 1993; WHEELOCK *et al.*, 1994; CROZAZ

127

Table 1. Minerals in enstatite chondrites and achondrites.

Mineral name	Chemical formula	Abundances (wt%)		
		EH3/4	EL5/6	Aubrites
Orthoenstatite	$Mg_2Si_2O_6$	46–52	62–67	77–97
Clinoenstatite	$Mg_2Si_2O_6$	trace	n.r.	trace
Diopside	$MgCaSi_2O_6$	trace	n.r.	0.2–7.8
Olivine	Mg_2SiO_4	trace	n.r.	0.3–9.8
Plagioclase	>Ab90	1.5–16	6.4–9.2	0.3–14
Roedderite	$(Na,K)_2Mg_5Si_{12}O_{30}$	trace	n.r.	trace
Quartz	SiO_2	trace	trace	trace
Cristobalite	SiO_2	1.5–4	n.r.	trace
Tridymite	SiO_2	trace	trace	n.r.
Fluor-Richterite	$Na_2CaMg_5Si_8O_{22}(F,OH)_2$	trace	n.r.	trace
Alabandite	$(Mn, Fe)S$	n.r.	0.25–0.4	0.25–0.4
Caswellsilverite	$NaCrS_2$	trace	n.r.	trace
Daubreelite	$FeCr_2S_4$	0–0.2	n.r.	trace
Djerfisherite	$K_3(Cu,Na)(Fe,Ni)_{12}(S,Cl)_{14}$	trace	n.r.	trace
Niningerite	$(Mg,Fe)S$	0.2–11.2	n.r.	n.r.
Oldhamite	CaS	<0.1–2	0.07–0.9	0–0.4
Sphalerite	ZnS	trace	trace	trace
Troilite	FeS	5.8–13	4.6–9.5	0.4–1.5
Heideite	$FeTi_2S_4$	n.r.	n.r.	trace
Cohenite	$(Fe,Ni)_3C$	trace	trace	n.r.
Kamacite	α-FeNi	17.5–23.8	13.3–24.2	0–2.47
Perryite	$(Ni,Fe)_5(Si,P)_2$	trace	trace	trace
Schreibersite	$(Fe,Ni)_3P$	0.1–1	0.66–1	trace
Taenite	γ-FeNi	trace	trace	trace
Graphite	C	0.03–0.6	0.1–0.4	trace
Lawrencite	$(Fe,Ni)Cl_2$	trace	n.r.	n.r.
Nierite	Si_3N_4	trace	n.r.	n.r.
Osbornite	TiN	trace	trace	trace
Sinoite	Si_2N_2O	n.r.	0–0.14	n.r.

trace: less than 0.1 wt%. n.r.: not reported. Data are compiled from KEIL (1968), WATTERS and PRINZ (1979) as well as many other sources.

and LUNDBERG, 1995). The high REE abundances and different REE abundance patterns in oldhamite in enstatite chondrites can be plausibly explained by condensation processes in a reduced solar gas (LARIMER *et al.*, 1984; LODDERS and FEGLEY, 1993). However, the origin of oldhamite in aubrites and the origin of its high REE content is still under debate (see below).

The aubrite parent body underwent igneous differentiation after metal and sulfides segregated from the silicates to form a core. The large crystal size of enstatite in some aubrites and the igneous texture of silicate assemblages indicate that some crystallization process took place on the aubrite parent body (*e.g.*, OKADA *et al.*, 1988). In order to model crystallization processes the REE distribution in aubritic minerals and the partition coefficients for the relevant mineral/melt systems need to be known.

Several measurements of REE abundances in bulk aubrites and in their individual mineral phases are available (*e.g.*, SCHMITT *et al.*, 1963; MASUDA, 1967; WOLF *et al.*,

1983; GRAHAM and HENDERSON, 1985; FLOSS and CROZAZ 1993; LODDERS et al., 1993; WHEELOCK et al., 1994). Likewise, the REE mineral/melt partition coefficients for pyroxene, olivine, diopside, and plagioclase are available (KENNEDY et al., 1993; GRUTZECK et al., 1974; DRAKE and WEILL, 1975). For modeling the igneous differentiation history of the aubrite parent body (APB) CaS/silicate partition coefficients are also needed, because the REE are strongly concentrated in oldhamite. Under highly reducing conditions the REE may not only partition between CaS and silicate but also between FeS and silicate. Some REE (and in particular Eu) may have been removed by an Fe-FeS melt during formation of the metal-sulfide core (LODDERS and PALME, 1989, 1990), which could explain the frequently observed negative Eu-anomaly in bulk aubrite samples (e.g., WOLF et al., 1983). To model this potential fractionation, REE FeS/silicate partition coefficients are also required.

The origin of oldhamite and its role during igneous differentiation is still unclear. Two different schools of thought exist on the origin of oldhamite in aubrites. One is that oldhamite crystallized from a melt during igneous differentiation on the aubrite parent body. Another is that oldhamite is a relict condensate, altered to a lesser or greater extent during igneous activity on the APB. The arguments pro and con for these opinions are summarized in the present paper. In addition, some properties of oldhamite and a model of the differentiation of the aubrite parent body are discussed.

2. Occurrence and Composition of Aubritic Oldhamite

2.1. Occurrence

In the brecciated aubrites, oldhamite mainly occurs as single grains in the matrix and is relatively easily identified by its pinkish color, or when weathered, greenish appearance. Most grains are ~100 μm to mm sized, but large grains up to 2 cm are occasionally observed (WHEELOCK et al., 1994). Other sulfides (e.g., troilite, alabandite) can be associated with oldhamite. In rare cases, oldhamite occurs as inclusions in pyroxene (FLOSS and CROZAZ, 1993; KURAT et al., 1992). It is interesting to note that most oldhamite occurs as individual grains and does not display eutectic textures when in association with other sulfides or metal, as might be expected if eutectic melting in the CaS-FeS-Fe system had occurred (VOGEL and HEUMANN, 1941).

The oldhamite often contains fine blebs of troilite and ferroan alabandite, which in turn may contain small inclusions or associations with caswellsilverite (LODDERS et al., 1993; WHEELOCK et al., 1994). The modal abundance of oldhamite is typically less than one percent and, because oldhamite easily decomposes by aqueous weathering, aubrite finds often do not contain any detectable oldhamite.

2.2. Major element composition of aubritic oldhamite and equilibration temperatures

The major element composition of oldhamite in aubrites is given by WATTERS and PRINZ (1979). Stoichiometric CaS contains 55.55 wt% Ca but oldhamite in aubrites contains only 52.0–54.8 wt% Ca because MnS (~1 wt% Mn) and MgS (~0.3 wt% Mg) are dissolved in CaS. The FeS content in oldhamite is generally very low (Fe < 0.02 wt%) in accord with CaS-FeS phase diagram studies by SKINNER and LUCE (1971), who found no detectable solid solution of FeS in CaS. A comparison of the Ca, Mg, and Mn content of
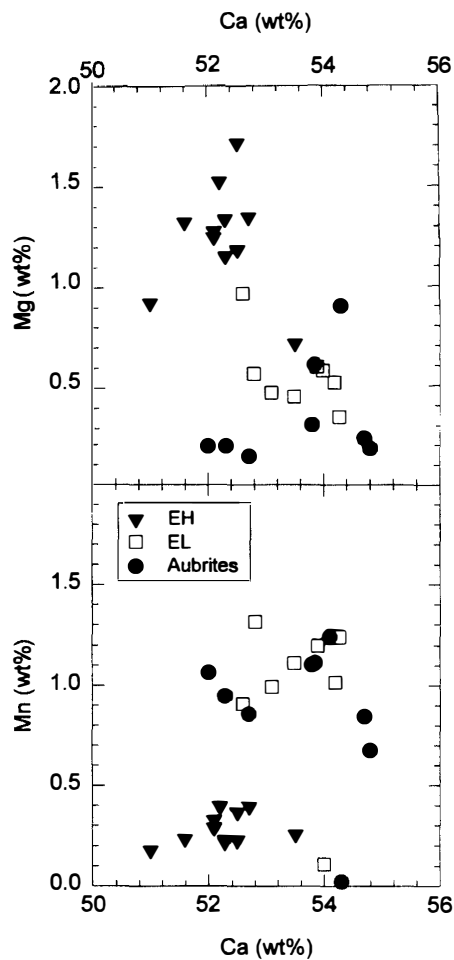
Fig. 1. Abundances of Mg, Mn, and Ca in oldhamite from enstatite chondrites and achondrites. The Mg content decreases and the Mn content increases from EH-chondrites to EL-chondrites to aubrites. Data from KEIL (1968), LARIMER and GANAPATHY (1987), LEITCH and SMITH (1982), WATTERS and PRINZ (1979), OKADA et al. (1988), LODDERS et al. (1993).

aubritic oldhamite and oldhamite in enstatite chondrites is given in Fig. 1. LARIMER and GANAPATHY (1987) pointed out that the Mn and Mg contents of oldhamite in enstatite chondrites reflect the degree of metamorphism. With increasing degree of metamorphism (i.e., increasing temperature), the Mn content increases and the Mg content decreases. The highest Mg content in oldhamite is found for the more primitive EH-chondrites, oldhamite in the more metamorphosed EL-chondrites has less Mg, and aubritic oldhamite is somewhat lower in Mg than EL-chondritic oldhamite. The inverse trend is observed for Mn in oldhamite, where EH-chondrites have the lowest Mn abundance and EL-chondrites and aubrites have higher and similar Mn contents.

One might expect that oldhamite of EL-chondrites and aubrites, which have experienced higher metamorphic temperatures than EH-chondrites, contains higher amounts of Mg, because the phase diagram studies by SKINNER and LUCE (1971) indicate a higher solubility of MgS in CaS at higher temperatures. However, in EL-chondrites and aubrites, niningerite ((Mg,Fe)S) is basically absent so that their study of MgS solubility in CaS for coexisting sulfides is not applicable. If niningerite were ever present in the EL-chondrite parent body or in the APB, the absence of niningerite in EL-chondrites and aubrites could be explained by oxidation of MgS by FeO or MnO from the silicates during metamorphic episodes.

SKINNER and LUCE (1971) developed the CaS-MnS-FeS geothermometer to determine the closure temperature of oldhamite in EL-chondrites. The similar compositions of EL-chondritic and aubritic oldhamite and the coexistence of small inclusions of troilite and alabandite in aubritic oldhamites allows us to apply the same geothermometer to aubrites (Fig. 2). Although REE distributions in aubritic minerals indicate that oldhamite is either partially or totally unequilibrated with respect to silicate phases (see below), we may assume that oldhamite is in local equilibrium with the associated sulfides and sulfide inclusions. The equilibration temperature can be calculated from:

$$T(^{\circ}C) = 603 + 13095 \cdot X_{MnS} - 119050 \cdot X^2_{MnS}, \tag{1}$$

where X_{MnS} is the mole fraction of MnS in CaS coexisting with MnS (alabandite) and FeS (troilite). The presence of less than 0.5 wt% Mg in most aubritic oldhamites (see Fig. 1) may have some effect on the solvus but was neglected here.

The minimum equilibration temperatures for aubrites, calculated for the average oldhamite composition given by WATTERS and PRINZ (1979), are between 700–800°C. The exception is the Pena Blanca Spring aubrite, for which Watters and Prinz report
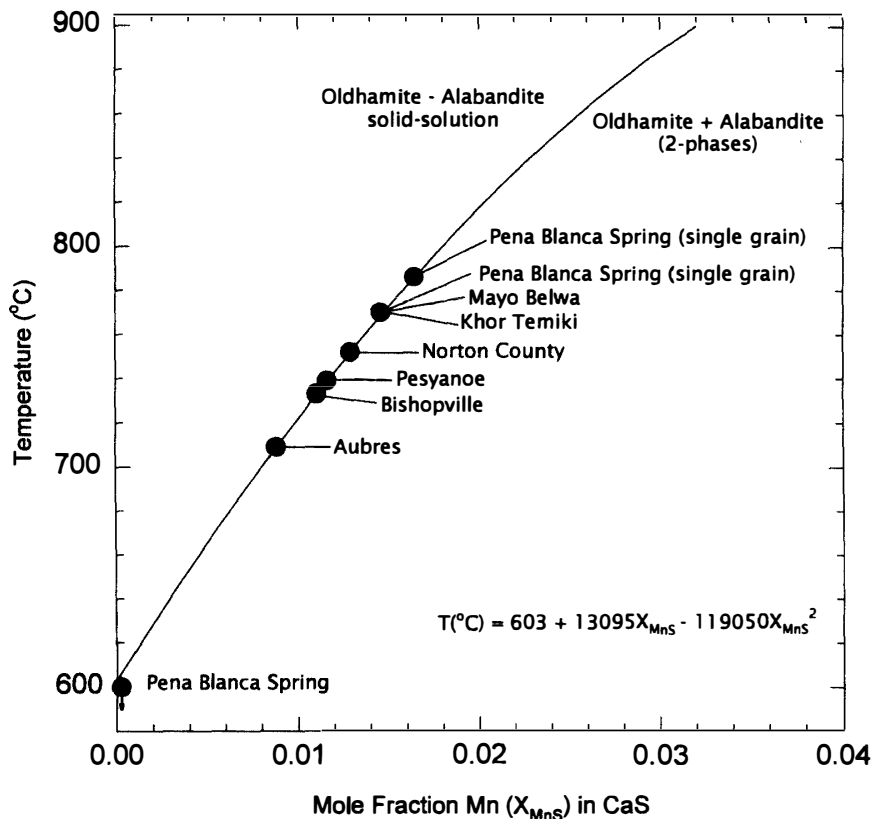

Fig. 2. Equilibration closure temperatures calculated with the CaS-MnS-FeS geothermometer of SKINNER and LUCE (1971). Data for aubritic oldhamite indicate equilibrium temperatures between 700 and 800°C. Data from WATTERS and PRINZ (1979), data for oldhamite single grains are from LODDERS et al. (1993).

<0.02 wt% Mn in oldhamite, which indicates closure of the CaS-MnS system below 600°C. However, the Mn content determined in two individual oldhamite grains from Pena Blanca Spring (LODDERS et al., 1993) yield 770 and 790°C, which fall into the general trend. It would be interesting to determine the equilibration temperatures for oldhamite grains displaying different REE abundance patterns (see next paragraphs) but unfortunately to date, no published ion probe analyses of meteoritic oldhamites have included major elements (e.g., Mg, Mn, Fe).

2.3. REE in oldhamite and other phases

The oldhamite from aubrites has been analyzed by several groups for trace elements, often with the main focus on the REE and actinides (MURRELL and BURNETT, 1982; BENJAMIN et al., 1984; FLOSS et al., 1990; KURAT et al., 1992; FLOSS and CROZAZ, 1993; LODDERS et al., 1993; WHEELOCK et al., 1994). REE and actinides abundances are generally about 50–200 times CI-chondritic, which implies that these elements are almost completely located in oldhamite, even though the modal abundance of oldhamite is about one percent or less. FLOSS and CROZAZ (1993) report ten different REE abundance patterns in aubritic oldhamite, and different patterns were even observed in oldhamites from the same meteorite.

Other REE bearing phases are albitic plagioclase with light REE abundances that are about 0.01–1 times CI-chondritic and Eu about 5–10 times CI, and diopside, which in most cases has a bow shaped REE pattern at about 0.1–10 times chondritic and an Eu-depletion. However, other patterns for diopside were also found (FLOSS and CROZAZ, 1993).

The high REE abundances and the diversity of REE patterns in oldhamite make representative sampling of the brecciated aubrites critical for determining the whole rock REE patterns in aubrites. The variety of bulk REE abundance patterns described in the literature (e.g., SCHMITT et al., 1963; MASUDA, 1967; WOLF et al., 1983) probably depends on how much oldhamite was present in each whole rock sample analyzed, on the REE abundance patterns in the oldhamites contained in the sample, and to some extent also on the amount of plagioclase present in the sample. An example of a mass-balance calculation to model bulk REE abundances is given by LODDERS et al. (1993) for the Pena Blanca Spring aubrite.

3. REE CaS/silicate and FeS/silicate Partition Coefficients: Experimental Data

As mentioned above, REE abundances in aubritic minerals and REE silicate/melt partition coefficients are both known. Other necessary data for modeling aubrite petrogenesis are CaS/melt and FeS/melt partition coefficients for the REE. These are discussed next. The experimental details are described elsewhere (LODDERS et al., 1990; LODDERS, 1991,1995) and here only a brief summary is given, together with a comparison of other experimental results from JONES and BOYNTON (1983) and DICKINSON et al. (1990a, b, 1991). FeS/silicate and CaS/silicate partition coefficients are shown in Figs. 3 and 4, and some experimental results are listed in Tables 2 and 3. The partition coefficients (D) are expressed as weight ratios of concentration in sulfide over concentration in silicate matrix.

Table 2. Experimental conditions, concentrations of REE in iron sulfide and silicate, and REE FeS/silicate partition coefficients (D) in runs containing Al-foil as an oxygen getter.

Run	EQ9[b]			EQ10[b]			EQ4			EQ3		
T(°C)	1200			1200			1200			1200		
Time(h)	5			5			2			2		
X_{FeO} (sil.)[a]	0.042			0.039			0.106			0.109		
log fO_2	−14.7			−14.8			−12.0			−12.3		
log fS_2	−5.8			−5.8			−4.4			−3.8		
	Fe-S	Sil.	D	Fe-S	Sil.	D	Fe-S	Sil.	D	Fe-S	Sil.	D
Fe wt%	62.33	3.68	16.9	61.0	3.59	17	66.11	9.57	6.9	64.89	9.73	6.7
Sc ppm	<0.2	25.6	<0.007	<0.085	24.2	<0.004	<0.12	20.7	<0.006	<0.09	21.9	<0.004
La ppm	41	140	0.29	74.1	156	0.48	0.28	195	0.0014	0.13	221	0.0006
Pr ppm	142	433	0.33	280	545	0.51	0.7	686	0.001	–	753	–
Nd ppm	80	326	0.25	205	536	0.38	<32	692	–	–	710	–
Sm ppm	4.7	27.9	0.17	8.8	43.3	0.20	0.028	38.2	0.0007	<0.012	34.6	<0.0004
Eu ppm	10.5	12.3	0.85	16.5	15.3	1.08	0.096	27.6	0.0035	0.12	40.4	0.003
Gd ppm	66	818	0.081	155	1080	0.14	<4	1120	<0.0036	–	1140	–
Tb ppm	10	162	0.062	21	222	0.094	<0.5	178	<0.0028	–	190	–
Dy ppm	2.6	44.7	0.058	3.1	37.8	0.082	<0.027	34	<0.0008	<0.03	40	<0.0007
Ho ppm	1.53	58.8	0.026	1.9	39.6	0.048	–	39	–	–	44.2	–
Yb ppm	5.7	175	0.033	5.7	181	0.032	<0.2	156	<0.0012	<0.14	161	<0.0009
Lu ppm	0.31	26.2	0.012	0.48	37.5	0.013	0.14	31.7	0.0044	<0.04	34.6	<0.001

INAA data (LODDERS, 1991). a: mole fraction FeO in silicate after the experiment. b: FeS exsolved from Si-bearing Fe-metal. – stands for not analyzed.

The REE FeS/silicate partition coefficients decrease from light to heavy REE, except for Eu, which partitions about ten times stronger into the sulfide than neighboring Sm or Gd (Fig. 3). This trend was found in all studies. However, JONES and BOYNTON (1983) report higher FeS/silicate partition coefficients than LODDERS (1991, 1995) or DICKINSON et al. (1990a, b, 1991). This may be due to different sulfide and silicate compositions or different redox conditions used in the experiments. Experiments conducted under more oxidizing conditions yield lower REE FeS/silicate partition coefficients than do reducing experiments where Al-foil was present as an oxygen getter (LODDERS, 1991, 1995). However, under reducing conditions appropriate to aubrite formation, the REE clearly develop chalcophile trends.

The determination of partitioning coefficients under reducing conditions is generally difficult. Two experimental approaches have been used to measure REE CaS/silicate partition coefficients. In the method used by JONES and BOYNTON (1983) and by DICKINSON et al. (1990a, b, 1991) a charge of REE-spiked silicates, FeS_2, and Mg or Al as a reducing agent was equilibrated in evacuated sealed silica tubes. In this system, a (Ca, Mg)S liquid is formed by sulfurization of the silicates. The resulting (Ca, Mg)S only contained up to 30 wt% Ca, which is much more Mg-rich than any oldhamite found in aubrites (Mg<1 wt%). In the method employed by LODDERS (LODDERS et al., 1990; LODDERS, 1991), a Ca-free but otherwise enstatite chondrite-like silicate, spiked with REE, was equilibrated with CaS in evacuated silica tubes. In these experiments, solid CaS equilibrates with liquid silicate and the resulting CaS (48–50 wt% Ca) contained only up to 5 wt%
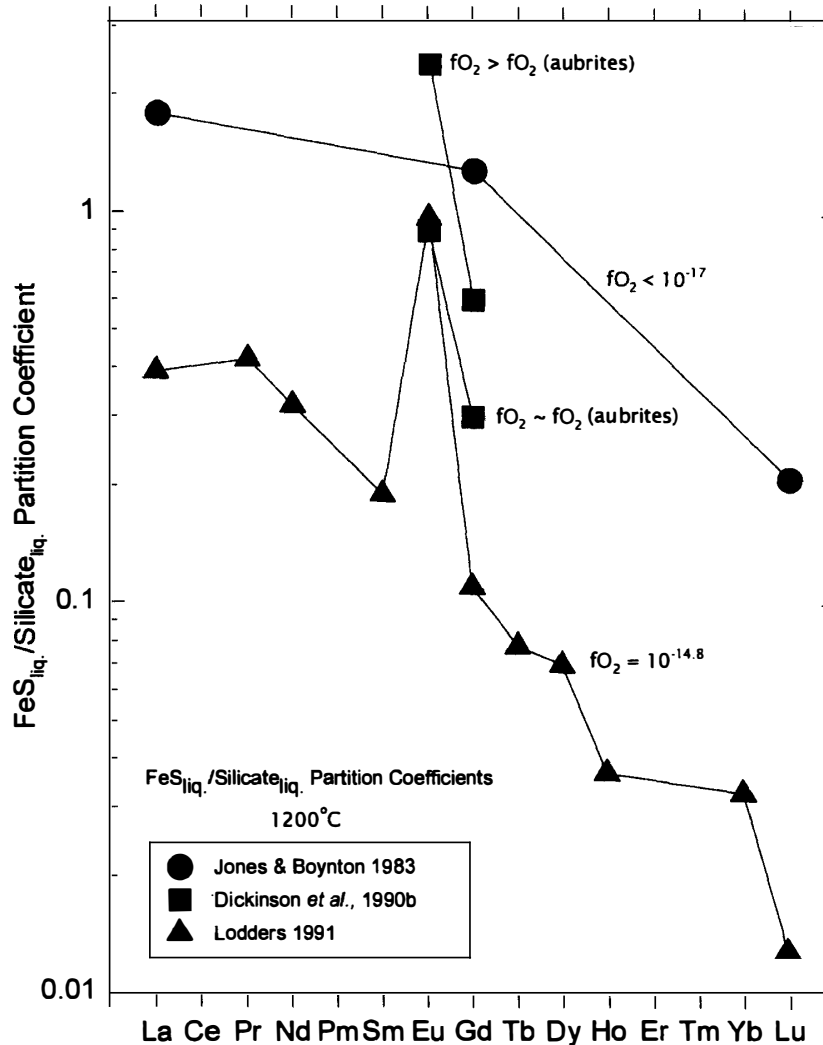
Fig. 3.   FeS/silicate partition coefficients for the REE at 1200 °C under reduc-
ing conditions. The oxygen fugacities prevailing during the experi-
ments are indicated in the graph. DICKINSON et al. (1990b) do not men-
tion which fO_2 they assume for aubrite formation. Assuming that an
fO_2 of 5 log units below the iron-wüstite buffer is representative for
aubrite formation, then fO_2 (aubrites) ~ 10^{-17} at 1200 °C.

Mg from exchange reactions with the silicate. However, the silicate matrix in the experi-
ments by LODDERS et al. (1990) contained up to 15 wt% CaO after the experiment, thus
making the silicate more calcic than bulk silicates observed in aubrites.

Since reaction times in silica tube experiments are limited by the stability of the
quartz glass at reaction temperatures, it was necessary to check if equilibrium was ob-
tained. Reversal experiments by LODDERS, using REE-spiked CaS and initially REE-free
silicate, gave somewhat higher CaS/silicate partition coefficients (about a factor of 2 for
Eu and ~4 for Sm and Gd, see Table 3). This indicates that equilibrium was not reached
within the duration of the experiments. Thus, results of the reversal experiments repre-
sent upper limits for REE partition coefficients between CaS and silicate melt. No rever-

Table 3. *Experimental conditions, concentrations of REE in CaS and silicate, and REE CaS/silicate partition coefficients.*

Run	CYA	CYC	CYB		CEI (rev.)	CEC	CEE	CEH (rev.)	CED[a]
T (°C)	1202	1306	1308		1202	1273	1295	1304	1308
Time(h)	18	21	20		18	16	16	22	26
wt%				Oldhamite					
Ca	51.80	48.67	47.46	Ca	49.31	50.31	49.91	48.53	52.97
Mg	1.76	4.4	4.83	Mg	0.11	2.27	2.40	3.62	0.46
Fe	0.30	0.92	1.04	Fe	0.37	0.69	0.88	0.92	1.88
Na	0.12	0.11	0.09	Na	0.10	0.08	0.09	0.19	0.09
S	42.36	43.52	43.17	S	43.64	41.23	41.70	44.75	44.58
La	0.39	0.15	0.21	Sm	0.75	0.53	0.55	0.79	0.42
Yb	0.43	0.46	0.52	Eu	0.83	0.68	0.78	1.04	0.49
Lu	0.39	0.42	0.45	Gd	0.71	0.48	0.51	0.99	0.41
sum[b]	97.55	98.65	97.77	sum[b]	95.82	96.27	96.82	100.8	101.3
wt%				Silicate matrix					
SiO_2	52.04	45.39	47.23	SiO_2	54.27	50.84	52.96	47.32	57.78
Al_2O_3	11.03	21.43	19.71	Al_2O_3	11.58	10.29	10.30	16.83	6.48
CaO	15.75	15.30	14.68	CaO	16.20	20.38	18.91	14.76	23.11
MgO	8.12	15.16	15.68	MgO	8.69	11.72	10.88	17.42	6.51
TiO_2	0.79	0.31	0.32	TiO_2	0.96	0.99	1.24	0.28	1.39
Na_2O	0.17	0.19	0.20	Na_2O	0.10	0.08	0.13	0.17	0.23
K_2O	0.18	0.16	0.18	K_2O	0.145	0.08	0.14	0.15	0.28
FeO	0.06	0.14	0.13	FeO	<0.03	0.18	0.14	0.10	0.59
La_2O_3	3.68	0.44	0.46	Sm_2O_3	2.15	1.83	1.88	0.75	0.89
Yb_2O_3	3.39	0.37	0.36	Eu_2O_3	0.52	0.68	0.80	0.56	0.50
Lu_2O_3	3.35	0.40	0.42	Gd_2O_3	2.29	1.69	1.76	0.92	0.98
sum	98.56	99.29	99.37	sum	96.91	98.76	99.14	99.26	98.74
D(La)	0.12	0.41	0.52	D(Sm)	0.45	0.34	0.34	1.23	0.55
D(Yb)	0.14	1.44	1.57	D(Eu)	1.87	1.13	1.14	2.16	1.14
D(Lu)	0.13	1.04	1.20	D(Gd)	0.36	0.33	0.34	1.24	0.48

Election Microprobe Analyses (LODDERS *et al.*, 1990). a: also contains coexisting FeS.
b: low totals due to surface oxidation. rev.: reversal experiment, REE initially contained in CaS.

sal experiments to test if equilibrium was achieved were published by JONES and BOYNTON (1983) or DICKINSON *et al.* (1990a, b, 1991). JONES and BOYNTON (1983) mention that their experimental charges probably are non-equilibrium assemblages, while DICKINSON *et al.* assume that equilibrium was reached between silicate liquid and immiscible sulfide liquid.

REE CaS/silicate partition coefficients are shown in Fig. 4. All groups investigating REE CaS/silicate partition coefficients found that partition coefficients increase from La to Lu (JONES and BOYNTON, 1983; DICKINSON *et al.*, 1990a, b, 1991; LODDERS *et al.*, 1990; LODDERS, 1991, 1995). However, absolute D values vary by about a factor of 20. These differences may be due to the different composition of the sulfide and silicate phases and may also be due to different oxygen and sulfur fugacities. The major difference in partitioning behavior was found for Eu. DICKINSON *et al.*(1990a, b, 1991) found that DEu for
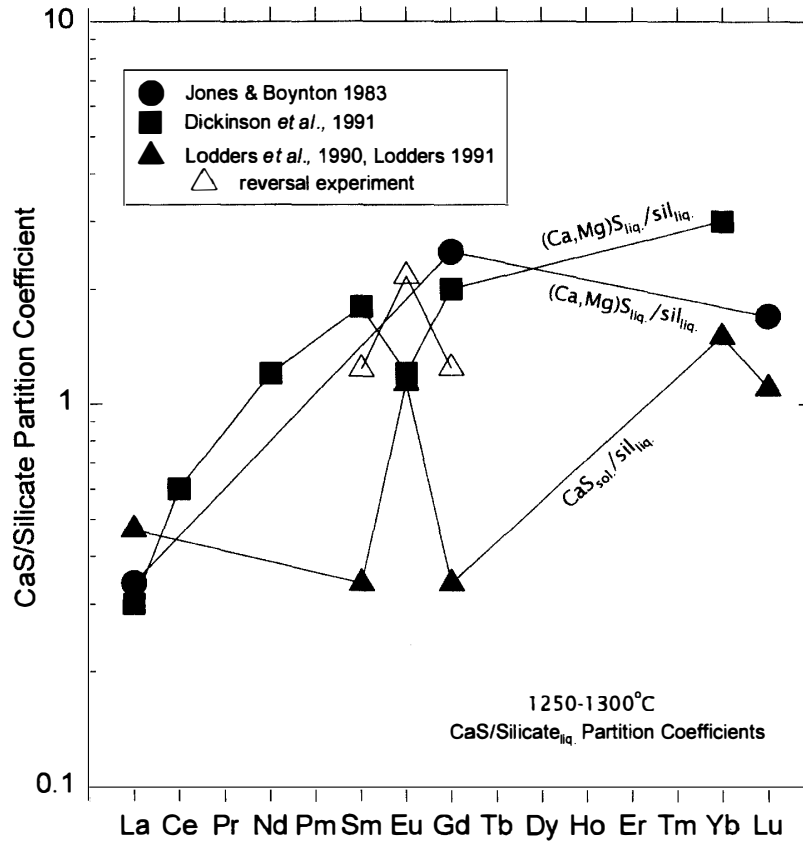
*Fig. 4.   CaS/silicate partition coefficients for the REE at 1250–1300°C un-
der reducing conditions. Experiments by JONES and BOYNTON and by
DICKINSON et al. led to formation of a (Ca,Mg)S liquid coexisting
with silicate melt while in experiments by LODDERS solid CaS coex-
isted with silicate melt. The Eu partition coefficient in the experi-
ments by DICKINSON et al. is lower than that of neighboring Sm or
Gd but the opposite is found in experiments by LODDERS. Reversal
experiments (open symbols), where the REE had to move from CaS
into silicate are 2–4 times higher than the partition coefficients
obtained from experiments where REE initially were contained in
the silicate, but also give DEu>DSm≈DGd. This indicates that equi-
librium was not reached, but the data from the reversal experiments
give upper limits to the partition coefficients. No reversal experi-
ments checking if equilibrium was obtained were published by JONES
and BOYNTON or DICKINSON et al.*

(Ca, Mg)S/silicate was smaller than D values for neighboring Sm and Gd. This behavior
of Eu is opposite to that found in the experiments by LODDERS et al. (1990) and LODDERS
(1991), where DEu>DSm≈DGd. The chemical behavior of Eu^{2+} is similar to that of Ca^{2+}
and Eu may be preferentially incorporated into Ca-rich, Mg-poor sulfides over Mg-rich,
Ca-poor sulfides. Experiments for REE FeS/silicate partitioning indicated that the parti-
tion coefficients depend on oxygen fugacity (see Fig. 3). DICKINSON et al. (1990b) also
found that the partition coefficients for the CaS/silictate system seem to depend on oxy-
gen fugacity. More experimental work is needed to investigate the REE partitioning as a

function of oxygen fugacity as well as of sulfide and silicate composition. However, all experimental results indicate that REE sulfide/silicate partition coefficients under reducing conditions are relatively small (D<10).

4. REE Distribution in Aubrites: Where did Oldhamite Originate?

To test if aubritic minerals, including oldhamite, are equilibrated with respect to REE and thus formed by crystallization processes, the REE concentration ratios in the mineral phases are compared to the respective partition coefficient ratios. A comparison of observed and predicted ratios is given in Fig. 5. The observed ratios were calculated
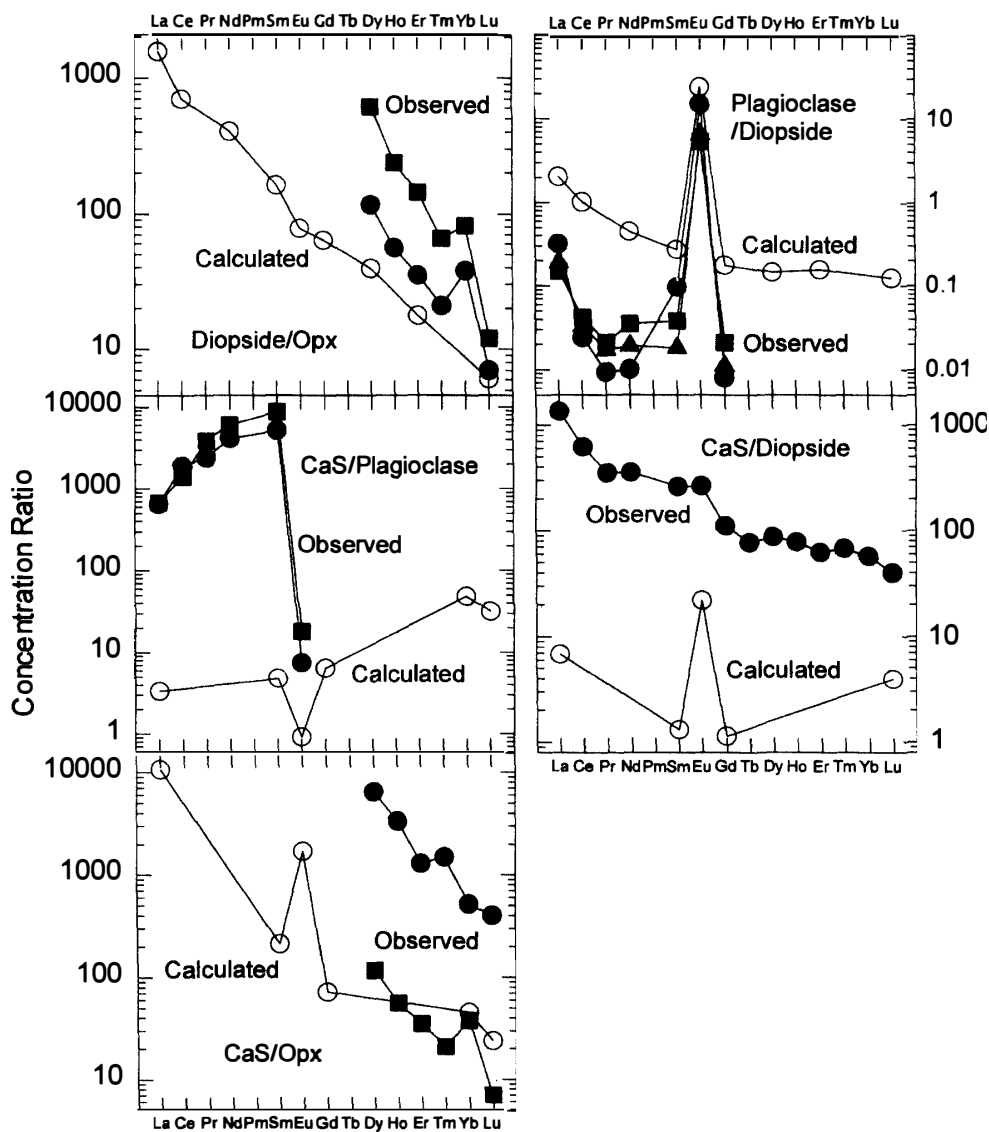
Fig. 5.   Observed REE concentration ratios in mineral pairs in aubrites and calculated ratios from partition coefficients. Observed and calculated ratios do not match, indicating that no co-crystallization took place on the APB. For data sources and more discussion see text.

using the REE measured concentrations in aubritic mineral phases (data from FLOSS and CROZAZ, 1993; WHEELOCK et al., 1994). Although oldhamite in aubrites displays a variety of patterns, the oldhamite pattern displaying a negative Eu anomaly was selected because this was observed in an oldhamite dominated clast in the Norton County aubrite (WHEELOCK et al., 1994). In this clast, oldhamite is apparently in igneous contact to other aubritic minerals so that it provides a good test if oldhamite and other aubritic minerals are in equilibrium with respect to REE.

The predicted REE ratios were calculated from the respective mineral/silicate liquid partitioning data (KENNEDY et al., 1993; GRUTZECK et al., 1974; DRAKE and WEILL, 1975) and CaS/silicate partition coefficients from LODDERS et al. (1990) and LODDERS (1991, 1995). Although the CaS/silicate partition coefficients may not represent equilibrium assemblages, the results of the reversal experiments give upper limits to the CaS/silicate partition coefficients. In addition, all studies show REE CaS/silicate partition coefficients of the same order of magnitude.

The observed and calculated ratios shown in Fig. 5 disagree indicating that the REE bearing minerals are not equilibrated. Thus, co-crystallization from a parent melt can be excluded, as also discussed by GRAHAM and HENDERSON (1985). The other possible crystallization process is fractional crystallization and subsequent removal of crystallized phases from the melt (OKADA et al., 1988). GRAHAM and HENDERSON (1985) concluded that a late crystallization of plagioclase in a fractional crystallization sequence is consistent with the REE distributions in the Mayo Belwa aubrite. However, the high REE concentrations in oldhamite are not explained by any of these crystallization processes.

In any crystallization sequence, the refractory (mp. 2450°C) oldhamite is expected to be among the first phases to crystallize, although it is not clear how CaS-rich oldhamite can crystallize from a Mg-rich melt. It has yet to be shown experimentally that Mg-poor oldhamite can form from an aubritic melt containing less than one percent Ca. The experiments by JONES and BOYNTON (1983) and DICKINSON et al. (1990a, b, 1991), where oldhamite was forced to form from a silicate melt by reaction with iron sulfide all yielded Mg-rich oldhamite.

Partition coefficients of about 100–200 are necessary to extract all REE from a melt into the small amount (~1 wt%) of oldhamite found in aubrites. However, the measured partition coefficients are about ≤ 10. If we assume that enstatite and olivine crystallize and CaS continues to equilibrate with the remaining melt, REE partitioning into CaS is more efficient. However, even in this case, neither the observed REE abundances in CaS nor the abundance patterns can be explained by partitioning. One could argue that the experimentally determined partition coefficients are too small because equilibrium was not reached between the CaS and silicate melt. However, the reversal experiments gave D values within a factor of 2–4 of the D values obtained from experiments with REE-doped silicate. Furthermore, the work by JONES and BOYNTON (1983) and DICKINSON et al. (1990a, b, 1991) also gave partition coefficients $\ll 100$. Thus, models postulating the efficient incorporation of REE into oldhamite from a silicate liquid are not supported by the available experimental data and appear extremely unlikely.

Another problem with crystallization processes is that they cannot explain the different REE patterns in oldhamite or diopside. At least 10 different types of patterns have been observed for oldhamite and at least three different patterns have been reported for

diopside (FLOSS and CROZAZ, 1993). LODDERS and PALME (1990) proposed that oldhamite in aubrites is a relict phase from the solar nebula. The diversity of REE patterns in aubritic oldhamite was later seen as an indicator of relict origin of oldhamite by other groups (FLOSS *et al.*, 1990; KURAT *et al.*, 1992; FLOSS and CROZAZ, 1993). The REE abundances and REE patterns in oldhamite from aubrites are similar to those in enstatite chondrites, which can be explained by REE condensation into oldhamite from a highly reduced nebular gas (LARIMER *et al.*, 1984; LODDERS and FEGLEY, 1993). Other indicators of the condensation origin of aubritic oldhamite are the mass independent sulfur isotopic anomalies observed by THIEMENS *et al.* (1994) because crystallization processes would isotopically equilibrate the anomalous sulfur in oldhamite with all the other isotopically 'normal' sulfur in the whole rock.

WHEELOCK *et al.* (1994) proposed that oldhamite in a oldhamite-dominated clast in Norton County crystallized from a melt and that the high REE abundances in the CaS resulted from equilibration with the aubritic melt. This suggestion is favored by the large (up to 2 cm) oldhamite crystal size, which is not easily explained by condensation processes. WHEELOCK *et al.* postulated the presence of a liquid CaS phase because forsterite grains are surrounded by oldhamite, and because rounded sulfide blebs occur in oldhamite. However, temperatures of about 2450°C are required for *liquid* CaS and even if melting point depression of CaS due to dissolved MnS, FeS, or MgS is considered temperatures above 2000°C are necessary (LODDERS *et al.*, 1993). It is doubtful if these temperatures were reached on the APB. High temperatures would also lead to substantial vaporization of *e.g.*, Na, K, Si, and Mg (FEGLEY and CAMERON, 1987). However, evaporative loss did not occur because aubrites still contain moderately volatile elements such as Na and K. Thus it is questionable that temperatures on the APB were high enough to melt oldhamite.

5. Preferred Differentiation Model of the Aubrite Parent Body and the Origin of Oldhamite

The aubrite parent body assembled from material compositionally similar to EH-chondrites (FOGEL *et al.*, 1988; LODDERS *et al.*, 1993). The REE are mainly located in oldhamite, which gained REE during condensation, as reflected by the diversity of its REE patterns and the high REE abundances. Impact melting led to heating and differentiation of the APB. Once temperatures reached ~1000°C, the Fe-FeS eutectic started segregating to form a core. Because oldhamite contains the REE and is not expected to be involved in major exchange reactions at these temperatures, the segregating FeS did not take up any significant amounts of REE. The low density of CaS (2.5 g/cm^3) allowed flotation and accumulation of small CaS grains once the silicates started melting. An example of such an accumulation process may be the CaS-rich 1.6 cm long impact melt vein in the Jajh deh Kot Lalu (EL6)-enstatite chondrite (RUBIN *et al.*, 1995). Once larger concentrations of CaS were produced, sintering led to larger CaS aggregates. Formation of larger CaS aggregates by sintering was observed in CaS/silicate partitioning experiments (LODDERS *et al.*, 1990; LODDERS, 1991). However, not all oldhamite inherited from the enstatite chondrite-like precursor may have come in contact with melt and accumulated. Most oldhamite in aubrites is small and comparable in grain size with that in enstatite chondrites (30–200 μm; LARIMER and GANAPATHY, 1987).

Lodders *et al.* (1993) previously proposed that the different REE patterns in diopside can be understood if diopside was formed from oldhamite. Fogel *et al.* (1988) suggested the reaction of oldhamite with enstatite to form diopside and forsterite. In that case, the diopside would inherit the REE inventory of the oldhamite. Floss and Crozaz (1993) report REE patterns in diopside, which contains a weathered oldhamite inclusion. This diopside may be the reaction product from oldhamite with enstatite, because its REE pattern is unlike those found in other diopsides in aubrites. This diopside shows two patterns with light REE around 0.5 times chondritic and heavy REE around 1 times chondritic. In addition, one pattern displays a small negative Eu anomaly. The oldhamite inclusion has a relatively flat pattern about 100 times chondritic. If diopside formed solely by crystallization from a melt, only the REE pattern expected from diopside/melt partitioning should be observed, instead of the different types of patterns which are actually found.

Crystallization processes also cannot explain the observed plagioclase zoning with anorthite at the rim and albite in the center, which was described by Wheelock *et al.* (1994) for an oldhamite dominated clast in the Norton County aubrite. Anorthite is more refractory than albite and crystallizes first. Thus a crystallization process predicts an anorthite rich interior and albitic rim instead. However, reaction of oldhamite with albite may explain the inverse zoning and also explain the negative Eu-anomaly in some aubritic oldhamites, because plagioclase favors the uptake of Eu over other REE.

It appears that the oldhamite from the precursor material of aubrites underwent different degrees of exchange reactions with its surrounding minerals but that these exchange reactions never reached equilibrium. These exchange process should also lead to zoning profiles in the REE distributions among minerals coexisting with CaS. Further REE measurements on such mineral assemblages may reveal that the REE underwent metamorphic redistribution. For example, preliminary ion probe investigations of enstatite in contact with oldhamite from the Pena Blanca Spring aubrite (Fahey *et al.*, 1995) show a falling concentration gradient of the REE from the oldhamite-enstatite interface towards the enstatite interior. Clearly more analytical work on aubrites and experimental work for modeling the behavior of REE among aubritic minerals is needed to understand the differentiation history of the APB.

Acknowledgments

References

Benjamin, T.M., Duffy, C.J., Maggiore, C.J. and Rogers, P.S.Z. (1984): Microprobe analyses of rare earth element fractionations in meteoritic minerals. Nucl. Instr. Meth. Phys. Res., **B3**, 677–680.

CROZAZ, G. and LUNDBERG, L.L. (1995): The origin of oldhamite in unequilibrated enstatite chondrites. Geochim. Cosmochim. Acta, **59**, 3817–3831.

DICKINSON, T.L., LOFGREN, G.E. and McKAY, G.A. (1990a): REE partitioning between silicate liquid and immiscible sulfide liquid: The origin of the negative Eu anomaly in aubrite sulfides. Lunar and Planetary Science XXI. Houston, Lunar Planet. Inst., 284–285.

DICKINSON, T.L., LOFGREN, G.E. and McKAY, G.A. (1990b): Sulfide fractionation and the origin of the negative Eu anomaly in aubrites. Meteoritics, **25**, 358.

DICKINSON, T.L., LOFGREN, G.E. and McKAY, G.A. (1991): On the magmatic origin of oldhamite in aubrites. Lunar and Planetary Science XXII. Houston, Lunar Planet. Inst., 319–320.

DRAKE, M.J. and WEILL, D.F. (1975): Partitioning of Sr, Ba, Ca, Y, Eu^{2+}, Eu^{3+}, and other REE between plagioclase feldspar and magmatic liquid: An experimental study. Geochim. Cosmochim. Acta, **39**, 689–712.

FAHEY, A., HUSS, G., WASSERBURG, G.J. and LODDERS, K. (1995): REE abundances and Cr isotopic composition of oldhamite and associated minerals from the Pena Blanca Spring aubrite. Lunar and Planetary Science XXVI. Houston, Lunar Planet. Inst., 385–386.

FEGLEY, B. and CAMERON, A.G.W. (1987): A vaporization model for iron/silicate fractionation in the Mercury protoplanet. Earth Planet. Sci. Lett., **82**, 207–222.

FLOSS, C. and CROZAZ, G. (1993): Heterogeneous REE patterns in oldhamite from aubrites: Their nature and origin. Geochim. Cosmochim. Acta, **57**, 4039–4057.

FLOSS, C., STRAIT, M.M. and CROZAZ, G. (1990): Rare earth elements and the petrogenesis of aubrites. Geochim. Cosmochim. Acta, **54**, 3553–3558.

FOGEL, R.A., HESS, P.C. and RUTHERFORD, M.J. (1988): The enstatite chondrite-achondrite link. Lunar and Planetary Science XIX. Houston, Lunar Planet. Inst., 342–343.

GRAHAM, A.L. and HENDERSON, P. (1985): Rare earth element abundances in separated phases of Mayo Belwa, an enstatite achondrite. Meteoritics, **20**, 141–149.

GRUTZECK, M., KRIDELBAUGH, S. and WEILL, D. (1974): The distribution of Sr and REE between diopside and silicate liquid. Geophys. Res. Lett., **1**, 273–275.

JONES, J.H. and BOYNTON, W.V. (1983): Experimental geochemistry in very reducing systems: Extreme REE fractionation by immiscible sulfide liquids. Lunar and Planetary Science XIV. Houston, Lunar Planet. Inst., 353–354.

KEIL, K. (1968): Mineralogical and chemical relationships among enstatite chondrites. J. Geophys. Res., **73**, 6945–6976.

KENNEDY, A.K., LOFGREN, G.E. and WASSERBURG, G.J. (1993): An experimental study of trace element partitioning between olivine, orthopyroxene and melt in chondrules: equilibrium values and kinetic effects. Earth Planet. Sci. Lett., **115**, 177–195.

KORNACKI, A.S. and FEGLEY, B. (1984): Origin of spinel-rich chondrules and inclusions in carbonaceous and ordinary chondrites. Proc. Lunar Planet. Sci. Conf., 14th, Pt. 2, B588-B596 (J. Geophys. Res., **89** Suppl.).

KORNACKI, A.S. and FEGLEY, B. (1986): The abundance and relative volatility of refractory trace elements in Allende Ca, Al-rich inclusions: Implications for chemical and physical processes in the solar nebula. Earth Planet. Sci. Lett., **79**, 217–234.

KURAT, G., ZINNER, E. and BRANDSTÄTTER, F. (1992): An ion microprobe study of an unique oldhamite-pyroxenite fragment from the Bustee aubrite. Meteoritics, **27**, 246–247.

LARIMER, J.W. (1975): The effect of C/O ratio on the condensation of planetary material. Geochim. Cosmochim. Acta, **39**, 389–392.

LARIMER, J.W. and BARTHOLOMAY, H.A. (1979): The role of carbon and oxygen in cosmic gases: some applications to the chemistry and mineralogy of enstatite chondrites. Geochim. Cosmochim. Acta, **43**, 1453–1466.

LARIMER, J.W. and GANAPATHY, R. (1987): The trace element chemistry of CaS in enstatite chondrites and some implications regarding its origin. Earth Planet. Sci. Lett., **15**, 123–134.

LARIMER J.W., BARTHOLOMAY, H.A. and FEGLEY, B. (1984): The chemistry of rare earth elements in the solar nebula. Meteoritics, **19**, 258.

LEITCH, C.A. and SMITH, J.V. (1982): Petrography, mineral chemistry and origin of type I enstatite chondrites.

Geochim. Cosmochim. Acta, **46**, 2083–2097.

LODDERS, K. (1991): Spurenelementverteilung zwischen Sulfid und Silikatschmelze und kosmochemische Anwendungen. Ph. D. Thesis, Univ. Mainz, Germany, 176p.

LODDERS, K. (1995): Experimental partitioning of rare earth elements between sulfides (FeS, CaS) and silicate melt and applications to enstatite achondrites. Antarctic Meteorites XX. Tokyo, Natl Inst. Polar Res., 140–143.

LODDERS, K. and FEGLEY, B. (1993): Lanthanide and actinide chemistry at high C/O ratios in the solar nebula. Earth Planet. Sci. Lett., **117**, 125–145.

LODDERS, K. and PALME, H. (1989): Europium anomaly produced by sulfide separation and implications for the formation of enstatite achondrites. Meteoritics, **24**, 293–294.

LODDERS, K. and PALME, H. (1990): Fractionation of REE during aubrite formation: The influence of FeS and CaS. Lunar and Planetary Science XXI. Houston, Lunar Planet. Inst., 710–711.

LODDERS, K. and PALME, H. (1991): Trace elements in mineral separates of the Pena Blanca Spring aubrite. Lunar and Planetary Science XXII. Houston, Lunar Planet. Inst., 821–822.

LODDERS, K., PALME, H. and DRAKE, M. J. (1990): The origin of oldhamite in enstatite achondrites (aubrites). EOS Trans. AGU, **71**, 1434.

LODDERS, K., PALME, H. and WLOTZKA, F. (1993): Trace elements in mineral separates of the Pena Blanca Spring aubrite: Implications for the evolution of the aubrite parent body. Meteoritics, **28**, 538–551.

MASON, B. (1966): The enstatite chondrites. Geochim. Cosmochim. Acta, **30**, 23–39.

MASUDA, M. (1967): Lanthanides in the Norton County achondrite. Geochem. J., **2**, 111–135.

MURRELL, M.T. and BURNETT, D.S. (1982): Actinide microdistributions in the enstatite meteorites. Geochim. Cosmochim. Acta, **46**, 2453–2460.

OKADA, A., KEIL, K., TAYLOR, G.J. and NEWSOM, H. (1988): Igneous history of the aubrite parent asteroid: Evidence from the Norton County enstatite achondrite. Meteoritics, **23**, 59–74.

RUBIN, A.E., SCOTT, E.R.D. and KEIL, K. (1995): Shock metamorphism of enstatite chondrites. Lunar and Planetary Science XXVI. Houston, Lunar Planet. Inst., 1197–1198.

SCHMITT, R.A., SMITH, R.H., LACH, J.E., MOSEN, A.W., OLEHEY, D.A. and VASILEVSKIS, J. (1963): Abundances of the fourteen rare-earth elements, scandium, and yttrium in meteoritic and terrestrial matter. Geochim. Cosmochim. Acta, **27**, 577–622.

SKINNER, B.J. and LUCE, F.D. (1971): Solid solutions of the type (Ca, Mg, Mn, Fe)S and their use as geothermometers for enstatite chondrites. Am. Mineral., **56**, 1269–1296.

THIEMENS, M.H., BREARLEY, A., JACKSON, T. and BOBIAS, G. (1994): Detection of a ^{35}S excess in an oldhamite separate from Norton County. Meteoritics, **29**, 540–541.

VOGEL, R. and HEUMANN, T. (1941): Das System Eisen-Eisensulfid-Kalziumsulfid. Archiv Eisenhüttenw., **15**, 195–199.

WATTERS, T.R. and PRINZ M. (1979): Aubrites: Their origin and relationship to enstatite chondrites. Proc. Lunar Planet. Sci. Conf., 10th, 1073–1093.

WHEELOCK, M.M., KEIL, K., FLOSS, C., TAYLOR, G.J. and CROZAZ, G. (1994): REE geochemistry of oldhamite-dominated clasts from the Norton County aubrite: Igneous formation of oldhamite. Geochim. Cosmochim. Acta, **58**, 449–458.

WOLF, R., EBIHARA, M., RICHTER, G. R. and ANDERS, E. (1983): Aubrites and diogenites: trace element clues to their origin. Geochim. Cosmochim. Acta, **47**, 2257–2270.